ON-WAFER MEASUREMENT AND MODELING OF MILLIMETER-WAVE GaAs SCHOTTKY MIXER DIODES

John L. Allen, Chun-Yao Chen, and David P. Klemer

NSF/Center for Advanced Electron Devices and Systems
Department of Electrical Engineering
The University of Texas at Arlington
Arlington, Texas 76019

ABSTRACT

Direct on-wafer U-band measurements of GaAs Schottky diodes have allowed for the development of bias-dependent nonlinear device models. The devices are low-parasitic-capacitance planar diodes [1,2], fabricated on epitaxial (n-on-n^+ GaAs) substrates prepared by metal-organic chemical vapor deposition. Schottky contacts with areas of 4 μm^2 and 9 μm^2 were formed using a Ti-Pt-Au metallization and plated airbridge contact technique [3]. Techniques evaluated for de-embedding device measurements involved both numerical simulation as well as a novel on-chip calibration procedure. Although this work considered Schottky diodes specifically, similar techniques could be employed for determining bias-dependent and large-signal models for the gate electrode of millimeter-wave MESFET and HEMT devices.

I. INTRODUCTION

Millimeter-wave Schottky mixer diodes having the device layout shown in Figure 1 were fabricated on epitaxial (n-on-n^+) gallium arsenide substrates prepared by metal-organic chemical vapor deposition (MOCVD); a scanning electron photomicrograph is also shown in Figure 1. The external contact configuration is a standard ground-signal-ground 50Ω coplanar waveguide arrangement to permit on-wafer characterization using 65 GHz wafer probes.

The gallium arsenide substrate material consisted of a 0.25μm n-layer of carrier concentration $1.5 \cdot 10^{17}$ cm^{-3}, above a 0.85μm n^+-layer of concentration $1.0 \cdot 10^{18}$ cm^{-3} (the devices were not of the Mott variety). The Schottky (anode) contact to GaAs, a Ti-Pt-Au metallization, terminates the central (signal) metallization using an air-bridge connection to minimize parasitic capacitance to the underlying n^+ region onto which the device cathode contact is made. Devices with anode areas of 4 and 9 μm^2 were available for testing. The coplanar waveguide transmission line between the physical device junction and point of probe contact is approximately 30 degrees in electrical length at 50 GHz.

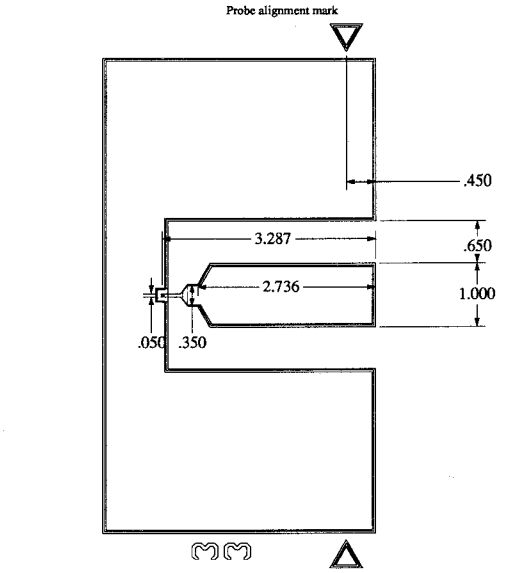

Figure 1. Mask layout and scanning electron photomicrograph of a schottky diode used for on-wafer characterization. (Values shown are actual dimensions (μm) ÷ 100.)

II. MEASUREMENTS

DC characterization of the devices was used to estimate diode ideality factor. An example current-voltage characterization of a typical device is given in Figure 2; ideality factors for the MOCVD devices were typically 2.0.

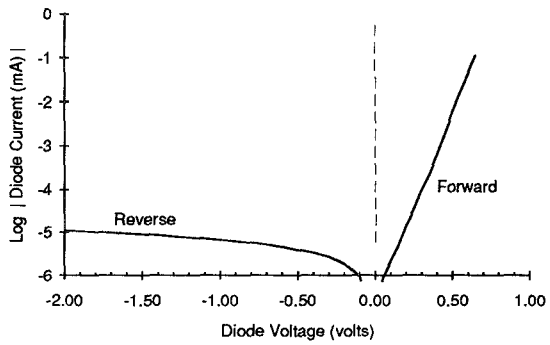

Figure 2. DC IV Characterization of an MOCVD Schottky Device.

RF (one-port) measurements of the devices were recorded across the 40-60 GHz waveguide band using Cascade Microtech 65 GHz wafer probes with DC bias supplied using external Wiltron 60 GHz bias tees. The measurement system was calibrated for one-port measurement at the wafer probe tip using the Cascade Microtech impedance standard substrate. Measurements were made at discrete frequencies across the 40-60 GHz band, with separate single-frequency calibration performed at each measurement point.

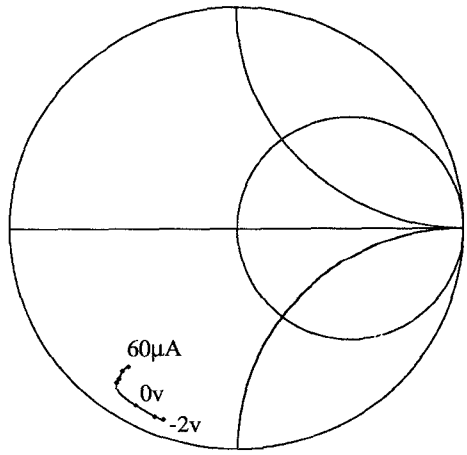

Figure 3. Swept-bias measurement at 52 GHz.

Figure 3 illustrates a small-signal impedance measurement of a Schottky device as DC bias is swept from -2 volts reverse bias to 60 μA forward bias (corresponding to a current density of 670 A/cm^2 for the 3-μm-square devices). The measurement in Figure 3 has not yet been de-embedded to the device junction; the reference plane is the point of probe contact.

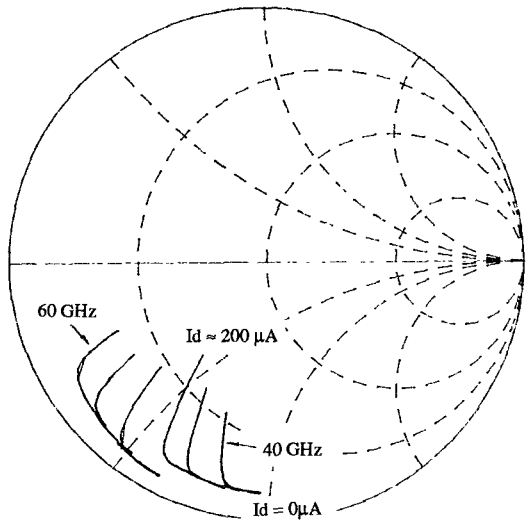

Figure 4. Swept-bias measurements over the 40-60 GHz band.

Figure 4 illustrates swept-bias data recorded for six frequencies from 40 to 60 GHz. In Figure 4, bias was changed from zero volts to a forward current of approximately 200 μA.

The device impedance data of Figure 4 can be plotted in the impedance plane as a function of bias and frequency. This has been done in Figure 5, with frequency varying from 40 to 60 GHz (in 4 GHz increments) and bias values ranging from 2 volts reverse bias to a forward current of 60 μA. The impedance values in Figure 5 represent embedded measurements, including the transmission line connecting the diode junction to the point of probe contact. The behavior is not unexpected—device reactance changes significantly in the reverse bias region as depletion region capacitance varies, and forward bias results in a change in device resistance and an accompanying increase in return loss.

An attempt to de-embed the measurements to the plane of the device junction was accomplished by on-chip calibration devices which were fabricated by gold-electroplating a short circuit from the diode anode to the nearby (cathode) ground metallization; measurements of this calibration device were used to estimate the phase length of the embedding coplanar transmission line as well as the associated loss. Unfortunately, this procedure yielded calculated phase lengths which were unrealistically long, likely due to parasitic reactance at a location near the device anode plane.

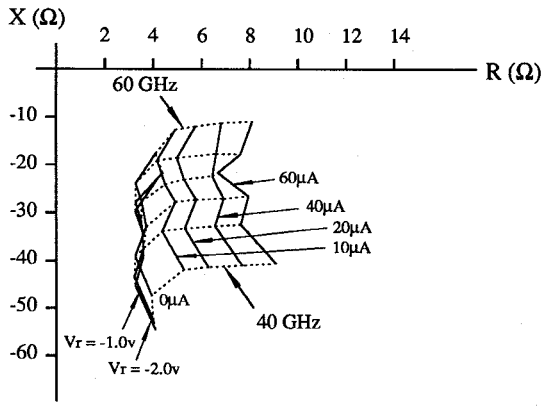

Figure 5. Device Impedance as a Function of Frequency and Bias.

An alternative approach for de-embedding used the fact that device capacitance is constant at a fixed bias. Small signal measurements were recorded over frequency and an appropriate length of lossless transmission line was subtracted from the embedded device data. The length of line was determined by calculating the capacitance at each frequency for the de-embedded data, and requiring that that capacitance value be constant for each data point. To facilitate this calculation, note that the reflection coefficient Γ_d associated with a lossless capacitance has a phase given by

$$\angle \Gamma_d(V_D) = \tan^{-1}\left(\frac{-2\,\omega\, C_j(V_D)\, Z_o}{1 - \omega^2\, C_j^2(V_D)\, Z_o^2}\right),$$

which allows $C_j(V_D)$ to be determined uniquely from the reflection coefficient. The proper length of embedding transmission line was determined as that which yields a de-embedded C_j value which is dependent on bias only, and not frequency.

Figure 6 illustrates a plot of calculated bias-dependent C_j values as a function of diode voltage calculated from the de-embedded impedance measurements of Figure 5. Also shown in Figure 6 is the small-signal circuit model of the Schottky device.

The series parasitic resistance R_s in the small-signal model cannot be estimated from DC measurements using the standard approach of Fukui [4] due to the very high (destructive) current densities involved. Instead, R_s is estimated as 5Ω from the constant-resistance arc along which the reverse-biased impedance measurements lie. Values for the forward-biased device conductance G_d are calculated by choosing appropriate values so as to fit model impedance to the de-embedded device measurement data. The alternative approach, where G_d is computed as an incremental conductance $G_d(V_d) = [dI_d/dV_d] = (qI_D/\eta kT)$, gives values which are unrealistically low, even if η is computed from actual DC measurement data.

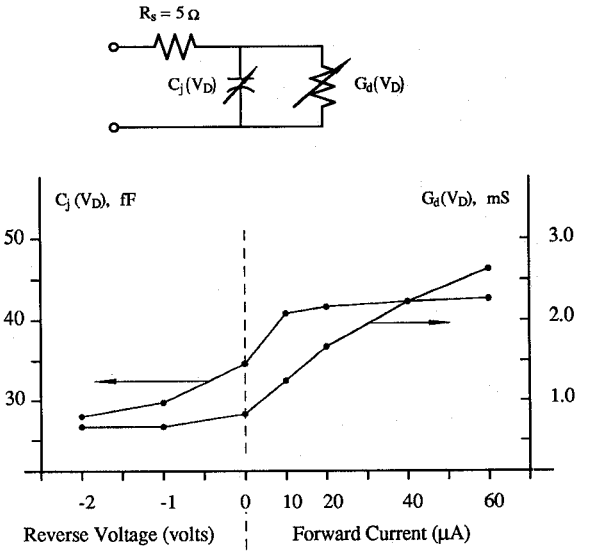

Figure 6. Device circuit model and variation of C_j and G_d as a function of device bias point.

Amplitude-dependent device models (or large-signal describing functions) can be developed in a similar manner. For example, Figure 7 illustrates the effect of RF amplitude on device impedance at 40, 52 and 60 GHz. The RF amplitude was increased by 16 dB from the small-signal measurement in Figure 7, and the diode was biased at 10 μA (with RF signal removed).

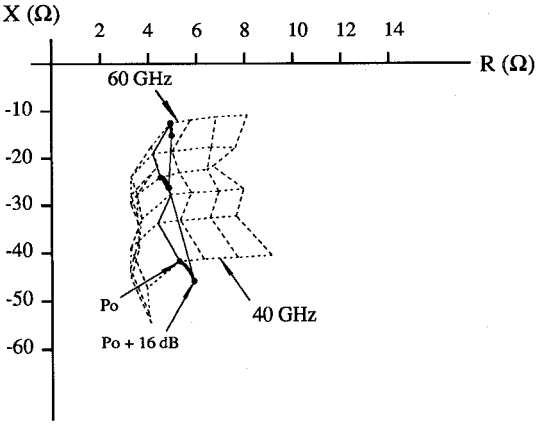

Figure 7. Effect of RF amplitude on device impedance at 40, 52 and 60 GHz

III. CONCLUSIONS

Direct on-wafer measurement of Ti-Pt-Au Schottky mixer diodes fabricated on GaAs MOCVD substrates have allowed for the development of bias-dependent small-signal models for these millimeter-wave devices. On-chip de-embedding structures and numerical procedures have been studied as approaches for de-embedding measurement data to the device junction. The techniques can be extended to study the effect of signal amplitude on device impedance.

IV. ACKNOWLEDGMENTS

The authors with to acknowledge and thank Mike Haji-Shiekh and Manisha Pujara for help with scanning electron microscopy. Thanks also to Cascade Microtech, Inc., Beaverton, Oregon, and to Bob M. Hawkins of Gamma Opt., Inc., Dallas, Texas, for equipment support which has greatly assisted in ongoing microwave and millimeter-wave measurement activities at The University of Texas at Arlington.

V. REFERENCES

[1] Bishop, W. L., K. McKinney, R. J. Mattauch, T. W. Crowe and G. Green, "A novel whiskerless Schottky diode for millimeter and submillimeter wave application," *1987 IEEE MTT-S Intl. Microwave Symp. Digest,* Las Vegas, June 1987, pp. 607-610.

[2] Archer, J. W., R. A. Batchelor and C. J. Smith, "Low-parasitic, planar Schottky diodes for millimeter-wave integrated circuits," *IEEE Trans. Microwave Theory and Techniques,* January 1990, pp. 15-22.

[3] Zych, D., J. Beall, D. Seymour, J. Delaney, B. Mercer, J. Stidham and M. Wdowik, "A GaAs vertical PIN diode production process," *1990 IEEE GaAs IC Symposium Digest,* New Orleans, October 1990, pp. 241-244.

[4] Fukui, H., "Determination of the basic device parameters of a GaAs MESFET," *Bell System Technical Journal,* March 1979, pp. 771-797.